ELSEVIER

Journal of Membrane Science 189 (2001) 179–191

journal of MEMBRANE SCIENCE

www.elsevier.nl/locate/memsci

Membrane-based Enthalpy Exchanger: material considerations and clarification of moisture resistance

J.L. Niu*, L.Z. Zhang

Department of Building Services Engineering, The Hong Kong Polytechnic University, Hung Hom, Kowloon, Hong Kong, China

Received 31 May 2000; received in revised form 15 November 2000; accepted 16 November 2000

Abstract

The fundamental dimensionless groups for coupled heat and moisture transfer in a cross flow air-to-air enthalpy exchanger with hydrophilic membrane cores are derived and validated with experimental data. The thermal and moisture transfer mechanisms in membranes are studied. The finite difference numerical solutions of the model are used to study heat and moisture transfer in enthalpy exchangers. The variations of sensible, latent, and enthalpy effectiveness with various operating parameters are calculated for different types of material. Studies show that the sensible effectiveness is mainly determined by number of transfer units (NTU) of the exchanger, while the latent effectiveness is influenced by both the material and the operating conditions. Unlike thermal diffusive resistance, the moisture diffusive resistance in membrane is not a constant. It is co-determined by the slopes of sorption curves and the operating conditions. To account for these influences, a new dimensionless factor named the coefficient of moisture diffusive resistance (CMDR) is defined. With this coefficient, the performance of an enthalpy exchanger can be more easily predicted and clearly understood. By comparing the performances with different membrane materials, it is revealed that the membrane material with a linear sorption curve performs better than other materials under common conditions.

Keywords: Micro-porous and porous membranes; Gas and vapor permeation; Dehumidification; Thermodynamics; Air conditioning

1. Introduction

Conditioning ventilation air typically constitutes 20–40% of the thermal load for commercial buildings and can be even higher in buildings that require 100% outdoor air to meet ventilation standards [1]. It is well known that energy recovery devices could save a large fraction of the thermal load since heat and humidity would be recovered from the exhaust stream in winter and excess heat and moisture would be transferred to the exhaust in order to cool and dehumidify the incoming air (supply) in the summer. With energy recovery devices, the efficiency of existing HVAC systems can also be improved because otherwise fresh air needs to be dehumidified by cooling coil through condensation followed by a re-heating process, which is very energy consuming.

The present techniques [2–6] for energy recovery can be classified into two categories: sensible heat exchangers and energy wheels. Sensible exchangers, such as fixed plates, sensible heat exchange wheels, heat pipes, and coil run-around loop heat exchangers, can only recover sensible heat with no moisture recovery. Energy wheels, which recover both heat and moisture, have a higher effectiveness, thus, are more attractive. However, energy wheels are very expensive

* Corresponding author. Tel.: +852-27667781; fax: +852-27746146.
E-mail address: bejlniu@polyu.edu.hk (J.L. Niu).

0376-7388/01/$ – see front matter
PII: S0376-7388(00)00680-3

Nomenclature

A	transfer area (m^2)
C	constant in sorption curve
c_p	specific heat ($kJ\,kg^{-1}\,K^{-1}$)
d_e	effective diameter of channel (m)
D_{va}	diffusivity of vapor in air ($m^2\,s^{-1}$)
D_{wm}	diffusivity of water in membrane ($kg\,m^{-1}\,s^{-1}$)
h	convective heat transfer coefficient ($kW\,m^{-2}\,K^{-1}$)
H	specific enthalpy ($kJ\,kg^{-1}$)
k	Convective mass transfer coefficient ($kg\,m^{-2}\,s^{-1}$)
$\dot{m}$	mass flow rate of air streams ($kg\,s^{-1}$)
$\dot{m}_W$	mass flow rate of moisture flow ($kg\,m^{-2}\,s^{-1}$)
n	number of channels
x, y, z	coordinates (m)
x^*, y^*, z^*	dimensionless coordinates
x_F	length of supply channel (m)
y_F	length of exhaust channel (m)
T	temperature (K)
u	velocity of air ($m\,s^{-1}$)
U	total heat transfer coefficient ($kW\,m^{-2}\,K^{-1}$)
w_{max}	maximum water uptake of desiccant ($kg\,kg^{-1}$)

Greek letters

ψ	coefficient of moisture diffusive resistance in membrane (CMDR)
λ	thermal conductivity of membrane ($kW\,m^{-1}\,K^{-1}$)
θ	moisture uptake in membrane ($kg\,kg^{-1}$)
ε	effectiveness
γ	resistance ($m^2\,K\,kW^{-1}$ for thermal and $m^2\,s\,kg^{-1}$ for moisture)
ϕ	relative humidity
δ	thickness of membrane (m)
ω	moisture content (kg moisture/kg dry air)
ρ	density ($kg\,m^{-3}$)

Subscripts

a	air
e	exhaust
i	inlet
L	latent, moisture
m	membrane
s	supply, sensible
o	outlet
w	water

and they have moving parts that may be problematic for maintenance. The carry-over is also a big problem.

Recently, Zhang et al. [7,8] proposed a new technique for energy recovery, namely, the enthalpy exchanger with hydrophilic membrane cores. Their device is just like an air-to-air sensible heat exchanger. But in place of traditional metal heat exchange plates, they utilize novel hydrophilic membranes, which can transfer both heat and moisture simultaneously. Preliminary results found that compared to an energy wheel, it has the same even higher enthalpy effectiveness. Furthermore, it is very easy to construct and implement, therefore, it is more promising and deserves further studying. The studies also found that unlike an energy wheel which usually has condensation and frost problems, there is hardly condensation and frost phenomenon for a membrane-based enthalpy exchanger, even at very extreme outside conditions. This is another superiority of membrane system.

Membrane materials, which are usually hydrophilic porous desiccants [9–13], have large impacts on the performance of enthalpy exchangers. This paper gives an investigation in this area. The effects of membrane material and outside operating conditions on the sensible, latent, and enthalpy effectiveness are discussed. Furthermore, to give a clearer insight into the moisture transfer mechanisms of the units, the moisture transfer resistance of membranes is separated and clarified, which leads to the definition and analysis of a new dimensionless factor, the so called coefficient of moisture diffusive resistance (CMDR).

2. The mathematical model

2.1. Governing equations

The governing equations for analyzing the coupled heat and moisture transfer in a membrane-based enthalpy exchanger are developed. The geometry of the

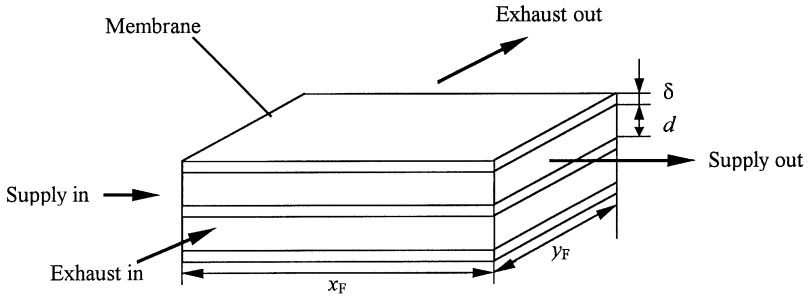

Fig. 1. Schematic of a cross-flow enthalpy exchanger with membrane cores.

device is shown in Fig. 1 in which the two air streams — the feed and the exhaust flow in thin, parallel, alternating membrane layers in a cross-flow arrangement, in order to transfer heat and moisture from one air stream to the other. For reasons of symmetry, the calculation domain is selected as the three-dimensional elementary cell in half the volume distributed between two consecutive layers.

The major assumptions in the mathematical model are summarized as follows:

1. Heat conduction and vapor diffusion of the two air streams along flow directions (axial) are negligible compared to energy transport and vapor convection by bulk flow.
2. Adsorption of water vapor and membrane material is in equilibrium adsorption-state.
3. Both the heat conductivity and the water diffusivity in the membrane are constants.
4. The heat of sorption is assumed constant and equal to the heat of vaporization.

The effect of axial fluid conduction/diffusion is totally negligible for Peclet number (*Pe*), $Pe = \rho_a u d_e/\lambda_a = 100$, and is quite small even for $Pe = 10$. In practical applications axial conduction/diffusion is frequently of considerable significance for laminar flow of liquid metals, which have very low Prandtl numbers. For gases, axial conduction/diffusion can be of importance only at extremely low Reynolds numbers [14]. Generally speaking, assumption (1) is valid when the Peclet number is bigger than 2.

Based on the above assumptions, the governing equations for the coupled heat and moisture transfer can be expressed as follows:

Supply:

$$\left(\frac{\dot{m}_s}{n_s y_F}\right) c_{ps} \frac{\partial T_s}{\partial x} + 2h_s(T_s - T_{ms}) = 0 \tag{1}$$

$$\left(\frac{\dot{m}_s}{n_s y_F}\right) \frac{\partial \omega_s}{\partial x} + 2k_s(\omega_s - \omega_{ms}) = 0 \tag{2}$$

Exhaust:

$$\left(\frac{\dot{m}_e}{n_e x_F}\right) c_{pe} \frac{\partial T_e}{\partial y} + 2h_e(T_e - T_{me}) = 0 \tag{3}$$

$$\left(\frac{\dot{m}_e}{n_e x_F}\right) \frac{\partial \omega_e}{\partial y} + 2k_e(\omega_e - \omega_{me}) = 0 \tag{4}$$

where T_{ms} and T_{me} are the temperature of membrane in supply side and exhaust side, respectively, ω the moisture uptake in air streams, x and y are coordinates, h the convective heat transfer coefficient, k the convective mass transfer coefficient, $\dot{m}$ mass flow rate of dry air, x_F and y_F are length of flow channels, n is the number of channels.

Membrane:

$$\dot{m}_w c_{pw} \frac{\partial T_m}{\partial z} - \lambda_m \frac{\partial^2 T_m}{\partial x^2} - \lambda_m \frac{\partial^2 T_m}{\partial y^2} - \lambda_m \frac{\partial^2 T_m}{\partial z^2} = 0 \tag{5}$$

$$\dot{m}_w = -D_{wm} \frac{\partial \theta}{\partial z} = D_{wm} \frac{\theta_{ms} - \theta_{me}}{\delta} \tag{6}$$

where θ_{ms}, θ_{me} are moisture uptake in membrane at two surfaces ($kg\,kg^{-1}$), δ the membrane thickness, D_{wm} the water diffusivity in membrane ($kg\,m^{-1}\,s^{-1}$), z is the coordinate in thickness direction (m).

2.2. Boundary conditions

Supply:

$$T_s|_{x=0} = T_{si} \tag{7}$$

$$\omega_s|_{x=0} = \omega_{si} \tag{8}$$

Exhaust:

$$T_e|_{y=0} = T_{ei} \tag{9}$$

$$\omega_e|_{y=0} = \omega_{ei} \tag{10}$$

Membrane:

$$\left.\frac{\partial T_m}{\partial x}\right|_{x=0} = 0 \tag{11}$$

$$\left.\frac{\partial T_m}{\partial x}\right|_{x=x_F} = 0 \tag{12}$$

$$\left.\frac{\partial T_m}{\partial y}\right|_{y=0} = 0 \tag{13}$$

$$\left.\frac{\partial T_m}{\partial y}\right|_{y=y_F} = 0 \tag{14}$$

Surface of membrane in supply side:

$$-\lambda_m \left.\frac{\partial T_m}{\partial z}\right|_{z=0} = h_s(T_s - T_m) + \dot{m}_w L_w \tag{15}$$

Surface of membrane in sweep side:

$$-\lambda_m \left.\frac{\partial T_m}{\partial z}\right|_{z=\delta} = -h_e(T_e - T_m) + \dot{m}_w L_w \tag{16}$$

where L_w is the latent heat of vaporization of water(kJ kg^{-1}).

It is well known that surface diffusion and capillary condensation with liquid flow are the predominant mechanisms of water vapor and air separation by porous solid membranes [15]. During the process of moisture permeation, the moisture is first adsorbed into one side of membrane, releasing heat. Under the driving force of concentration gradients in membrane, the adsorbed water is then transported to the other side of membrane, and desorbs while absorbing heat.

The equilibrium between the membrane and moisture at its surface can be expressed with a general sorption curve as [4]

$$\theta = \frac{w_{max}}{1 - C + C/\phi} \tag{17}$$

where w_{max} represents the maximum moisture content of the membrane material (i.e. moisture uptake when $\phi = 100\%$) and C determines the shape of the curve and the type of sorption. Fig. 2 shows the sorption curves for different C values. The most commonly used desiccants are: silica gel, linear-type, $C = 1$; molecule sieve, type-I, $C = 0.1$; polymers, type-III, $C = 10$.

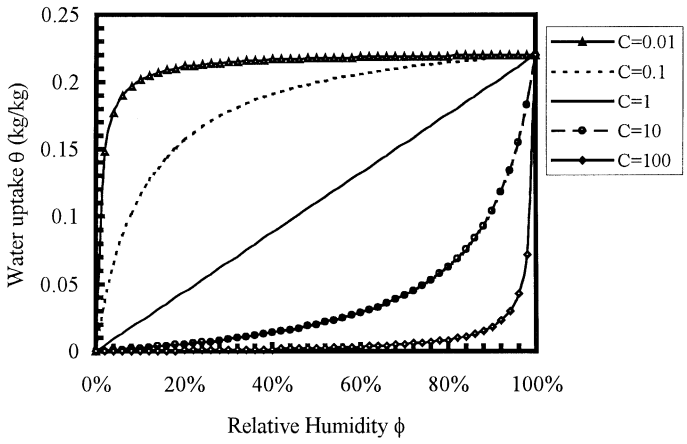

Fig. 2. Typical sorption curves for various membrane materials.

The relative humidity

$$\phi = \frac{P_v}{P_{satu}} \tag{18}$$

where P_{satu} is the saturation pressure of vapor in air (Pa). The relation between P_v and total pressure of atmosphere P is calculated by

$$P_v = \frac{\omega P}{\omega + 0.622} \tag{19}$$

The convective heat transfer coefficient is represented by a Nusselt number

$$Nu = \frac{h}{d_e} \tag{20}$$

or a Stanton number for heat transfer

$$St_H = \frac{h}{\rho_a c_p u} \tag{21}$$

where u is air stream bulk velocity ($m\,s^{-1}$), d_e is the effective diameter of the flow channel (m).

The Chilton–Colburn j factor for heat transfer [16]

$$j_H = St_H Pr^{2/3} \tag{22}$$

where Pr is the Prandtl number of moisture air.

Mass transfer in boundary layers is often described by a Sherwood number

$$Sh = \frac{kd_e}{D_{va}} \tag{23}$$

or a Stanton number for mass transfer

$$St_L = \frac{k}{\rho_a u} \tag{24}$$

The Chilton–Colburn j factor for mass transfer

$$j_L = St_L Sc^{2/3} \tag{25}$$

where Sc is the Schmidt number of moisture air.

By using the well known Chilton–Colburn analogy [16], we have

$$j_H = j_L \tag{26}$$

Substituting Eq. (20) through (25) into (26), a relation can be obtained

$$Sh = Nu \cdot Le^{-1/3} \tag{27}$$

$$Le = \frac{Pr}{Sc} \tag{28}$$

where Le is commonly called the Lewis number. For ventilation air and vapor mixture, which is always near atmospheric states, the Lewis number varies in the range of 1.19–1.22, see [14].

2.3. Normalization of equations

A set of simplified dimensionless equations can be further developed from the above governing equations as follows:

Supply:

$$\frac{\partial T_s}{\partial x*} = 2NTU_s(T_m - T_s) \tag{29}$$

$$\frac{\partial \omega_s}{\partial x*} = 2NTU_{Ls}(\omega_{ms} - \omega_s) \tag{30}$$

Exhaust:

$$\frac{\partial T_e}{\partial y*} = 2NTU_e(T_m - T_e) \tag{31}$$

$$\frac{\partial \omega_e}{\partial y*} = 2NTU_{Le}(\omega_{me} - \omega_e) \tag{32}$$

Membrane:

$$\frac{\partial T_m}{\partial z*} = a_1 \frac{\partial^2 T_m}{\partial x*^2} + a_2 \frac{\partial^2 T_m}{\partial y*^2} + a_3 \frac{\partial^2 T_m}{\partial z*^2} \tag{33}$$

where

$$x* = \frac{x}{x_F} \qquad y* = \frac{y}{y_F} \qquad z* = \frac{z}{\delta}$$

$$a_1 = \frac{\lambda_m \delta}{\dot{m}_W c_{pw} x_F^2} \qquad a_2 = \frac{\lambda_m \delta}{\dot{m}_W c_{pw} y_F^2}$$

$$a_3 = \frac{\lambda_m}{\dot{m}_W c_{pw} \delta}$$

$$NTU_s = \frac{n_s h_s x_F y_F}{\dot{m}_s c_{ps}} = \frac{h_s A_{tot}}{\dot{m}_s c_{ps}}$$

$$NTU_e = \frac{n_e h_e x_F y_F}{\dot{m}_e c_{pe}} = \frac{h_e A_{tot}}{\dot{m}_e c_{pe}}$$

$$NTU_{Ls} = \frac{k_s A_{tot}}{\dot{m}_s} \qquad NTU_{Le} = \frac{k_e A_{tot}}{\dot{m}_e}$$

$$\frac{\mathrm{NTU}}{\mathrm{NTU_L}} = \frac{h}{kc_p}$$

The above dimensionless parameters are the commonly recognized NTU. They give an insight into the characteristics of heat and moisture exchange between fluids and surfaces. Note that the supply and exhaust sides of the heat exchanger may have different heat transfer coefficients or surface areas, so a total number of transfer units is used to reflect the heat and moisture transfer in an exchanger. For the membrane exchanger that has equal area on both sides, the total number of transfer units is

$$\mathrm{NTU}_0 = \frac{A_{\mathrm{tot}} U}{(\dot{m} c_p)_{\min}} \tag{34}$$

where U is the total heat transfer coefficient.

$$U = \left[\frac{1}{h_s} + \frac{\delta}{\lambda} + \frac{1}{h_e} \right]^{-1} \tag{35}$$

The term in the middle is the thermal resistance of membrane, which is very small compared to the convective resistance and can be neglected. In the case of equal convective heat transfer coefficients on the two sides of membrane, NTU_0 becomes simply

$$\mathrm{NTU}_0 = \frac{\mathrm{NTU_s}}{2} = \frac{\mathrm{NTU_e}}{2} \tag{36}$$

Similar to the definition of total number of transfer units for heat, the total number of transfer units for moisture can be written as

$$\mathrm{NTU_{L0}} = \frac{A_{\mathrm{tot}} U_L}{(\dot{m})_{\min}} \tag{37}$$

where U_L is the total mass transfer coefficient.

2.4. Definition of effectiveness

Sensible heat transfer effectiveness

$$\varepsilon_s = \frac{\dot{m}_s (T_{si} - T_{so}) + \dot{m}_e (T_{eo} - T_{ei})}{2\dot{m}_{\min} (T_{si} - T_{ei})} \tag{38}$$

Latent heat transfer effectiveness, assuming the enthalpy of phase change is constant

$$\varepsilon_L = \frac{\dot{m}_s (\omega_{si} - \omega_{so}) + \dot{m}_e (\omega_{eo} - \omega_{ei})}{2\dot{m}_{\min} (\omega_{si} - \omega_{ei})} \tag{39}$$

Enthalpy transfer effectiveness, i.e. total energy transfer effectiveness

$$\varepsilon_{\mathrm{tot}} = \frac{\dot{m}_s (H_{si} - H_{so}) + \dot{m}_e (H_{eo} - H_{ei})}{2\dot{m}_{\min} (H_{si} - H_{ei})} \tag{40}$$

3. Results and discussion

3.1. Numerical solution of the model and validation

A finite difference technique is used to calculate the performance. The calculating domain is divided into a number of discrete nodes. Each node represents a control volume. The numbers of the calculating nodes are 100, 100, and 20 in x, y and z directions, respectively. For air streams, an upstream differencing scheme is used and for membrane, a central-difference operator is used.

The model has been validated by the experimental data of a cross-flow membrane-based enthalpy exchanger that is built for experimental and numerical studies [7]. In this study, a new type of membrane material that has a typical III class sorption curve is used as the core. Some parameters for the exchanger studied in this case are listed in Table 1. The comparisons between the simulated and the test results are shown in Figs. 3 and 4 for sensible and latent effectiveness, respectively. The maximum uncertainties for the tested sensible effectiveness are: 16.8% for air mass flow rate of $0.01\,\mathrm{kg\,s^{-1}}$ and 12.2% for $0.05\,\mathrm{kg\,s^{-1}}$ flow rate, respectively. The maximum uncertainties for the latent effectiveness are 9.8% for air mass flow rate of $0.01\,\mathrm{kg\,s^{-1}}$ and 5.2% for $0.05\,\mathrm{kg\,s^{-1}}$, respectively. A large fraction of the uncertainties came from the uncertainties in air-flow-rate measurement. However, for

Table 1
Some parameters of the membrane-based enthalpy exchanger for model validation

Symbol	Value
D_{wm}	2.16E-8 ($\mathrm{kg\,m^{-1}\,s^{-1}}$)
$w_{\max}$	0.23 ($\mathrm{kg\,kg^{-1}}$)
x_F	0.5 (m)
y_F	0.5 (m)
δ	20 (μm)
n_s	15
n_e	15
C	2.5 (III-type)

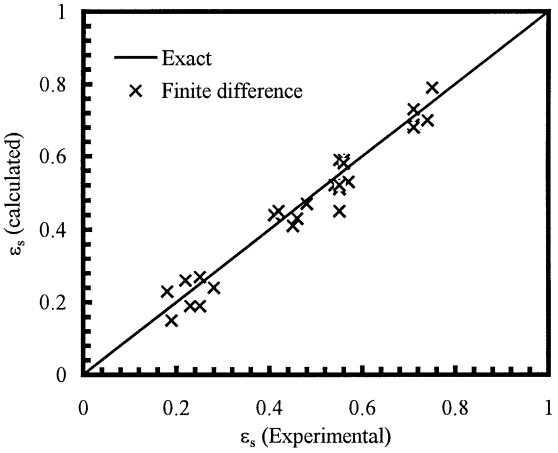

Fig. 3. Comparisons of sensible effectiveness experimental and calculated.

most of the test results, the uncertainties are less than 5% because most of the temperature differences between the two inlets are bigger than 1.5°C and/or the humidity differences are greater than 3.4 g kg^{-1}. From these two figures, it is concluded that the model predicts the effectiveness well and it can be used to study the performance of exchanger with membrane cores.

Since the flow arrangement is in a cross-flow, both the supply and the exhaust air streams are two-dimensional for temperature and humidity distributions. Figs. 5 and 6 show the distributions of temperature (a); and humidity (b) of supply air and

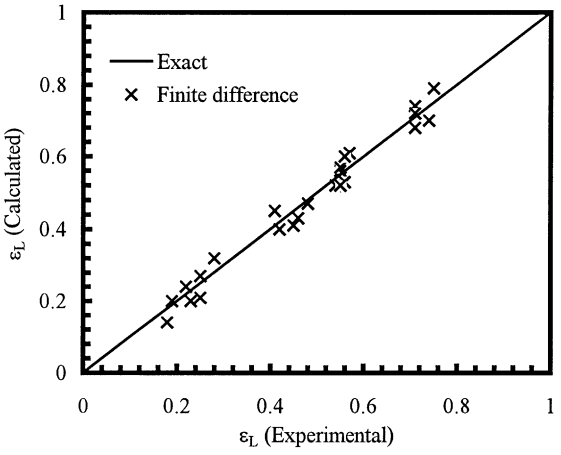

Fig. 4. Comparisons of latent effectiveness experimental and calculated.

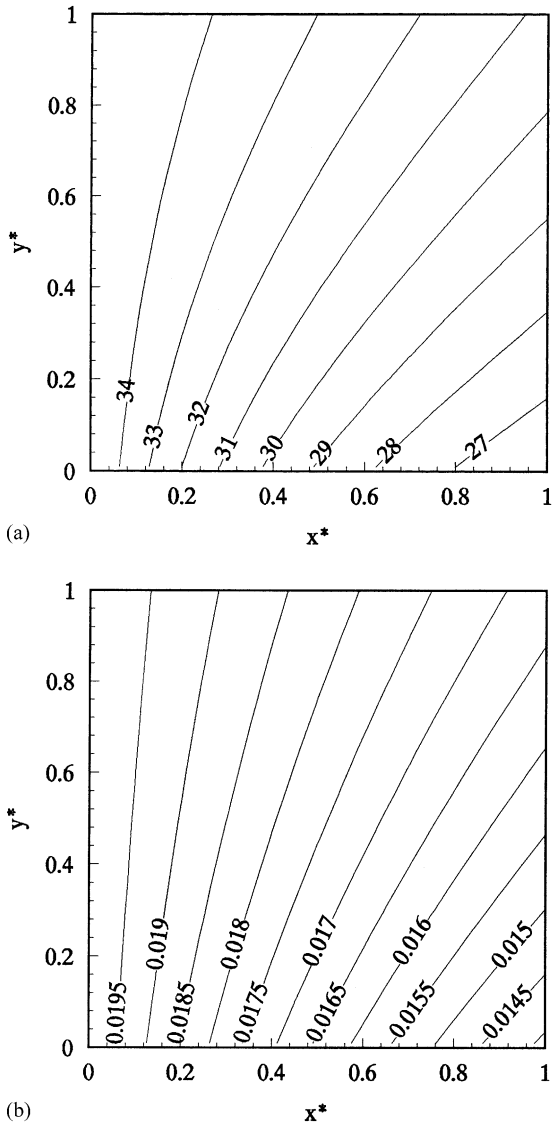

Fig. 5. (a) Temperature distribution of supply air stream (°C), inlet 35.07°C; (b) humidity distribution of supply air stream (kg kg^{-1}), inlet 0.01966 kg kg^{-1}.

exhaust air, respectively. Fig. 7 shows the temperature field of membrane. Due to the small thickness of membrane, the temperature differences of membrane in thickness are very small compared to those in x and y directions. Thus, heat conduction in membrane can be assumed one-dimensional (in thickness direction). The variations of temperature (humidity) difference between the two sides of membrane are mainly caused

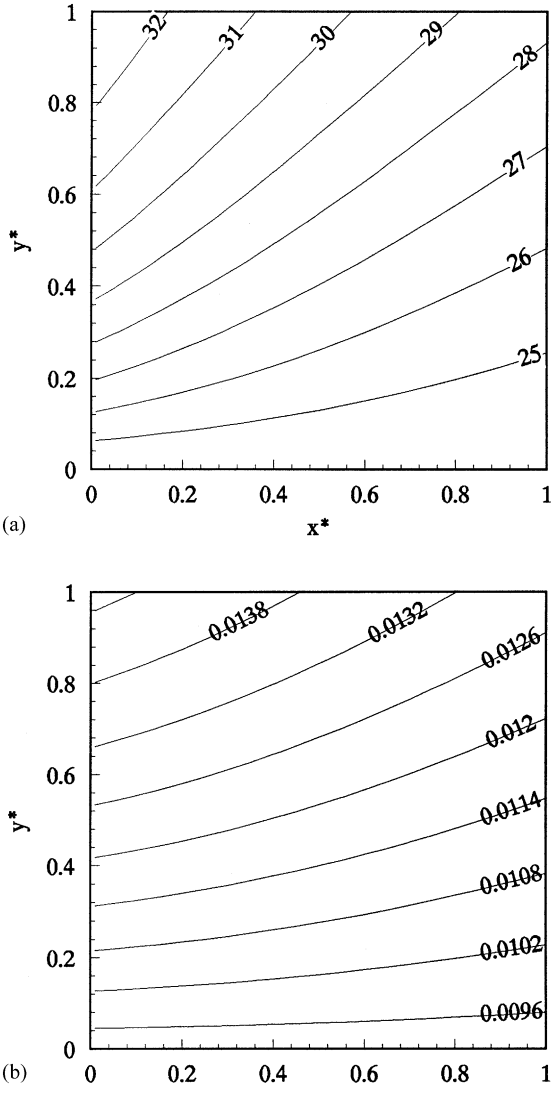

Fig. 6. (a) Temperature distribution of exhaust air stream (°C), inlet 24.83°C; (b) humidity distribution of exhaust air stream (kg kg^{-1}), inlet 0.00902 kg kg^{-1}.

by the variations of temperature (humidity) difference between the two air streams.

3.2. Effectiveness variations due to different design and operating conditions

3.2.1. Effects of NTU

The effectiveness is seriously influenced by the operating conditions. The Effects of total heat transfer

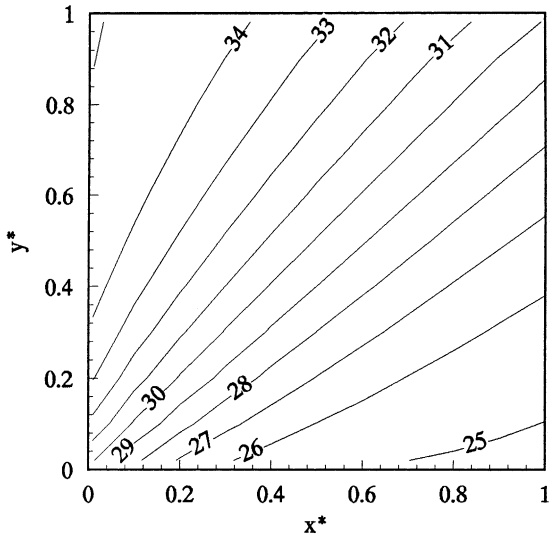

Fig. 7. Temperature distribution in the membrane (°C).

units on the sensible effectiveness, latent effectiveness and enthalpy effectiveness are shown in Fig. 8. NTU_0 is changed numerically by changing the convective heat transfer coefficients, the transfer area, and the mass flow rate of dry air from the base parameters shown in Table 1. As can be seen, ε_s, ε_L, and ε_{tot} all increase with an increasing NTU_0, but they increase more rapidly when the NTU_0 is in the range of 0–5. The sensible effectiveness is larger than the latent effectiveness regardless of NTU_0.

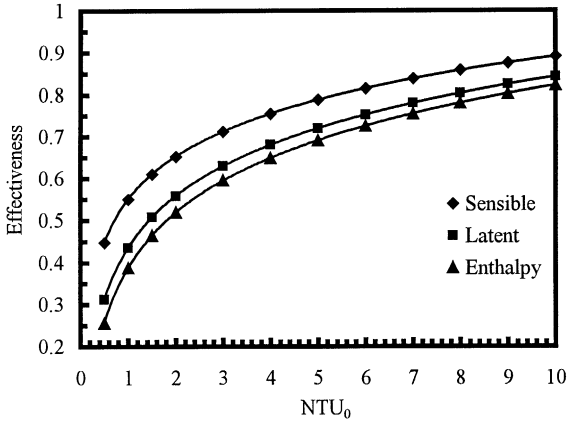

Fig. 8. The Effects of total number of heat transfer units on the effectiveness.

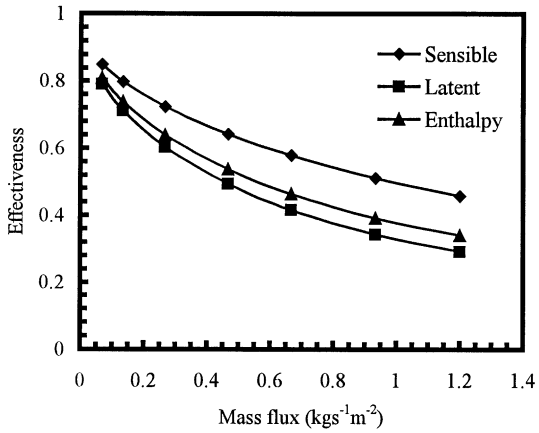

Fig. 9. Effects of mass flux of air streams on the effectiveness.

3.2.2. *Effects of air flow rates*

The mass flow rates of air streams have a big influence on the effectiveness. This can be seen from Fig. 9, in which a balanced flow (the air mass flow rates are the same for both the supply and the exhaust). The sensible, latent, and total enthalpy effectiveness decrease when the mass flux is increased. This is due to the decrease in NTU_0 with increasing mass flow rate. When the mass flow rate is increased, although the convective heat and mass transfer coefficients tend to increase, which will lead to a bigger effectiveness, the total number of transfer units and the effectiveness will be smaller. For a given dimension, trying to increase the package density of membrane is a good way to realize high performance of the exchanger.

3.2.3. *Effects of inlet humidity*

The effects of the inlet states of the supply air on the effectiveness of the exchanger are simulated with various membrane materials. The simulations are conducted with constant exhaust inlet condition (24°C and 50% RH). The inlet state of supply air has little effects on the sensible effectiveness. But it has a big impact on the latent effectiveness. The results in Fig. 10 show a wide range of latent effectiveness values for different membrane materials with different sorption curves and supply air inlet humidities. The latent effectiveness keeps almost constant for linear sorption membrane, but it decreases rapidly as the supply air becomes more humid for type-I sorption membrane material. The trend for type-III membrane material is opposite to that for type-I material. This indicates that a better performance could be obtained with type-I membrane when supply is dry, and with type-III if it is humid. The best performance could be easily realized with a linear-type membrane, regardless of inlet conditions. These performance differences can be better explained by the different slopes of their sorption curves (in Fig. 2). When the relative humidity is smaller than 50%, the slope of sorption curve for type-I material is steeper than that for type-III material. When the relative humidity is bigger than 50%, the slope for the latter one is steeper. On the other hand, the slope of the linear sorption curve does not change and is always

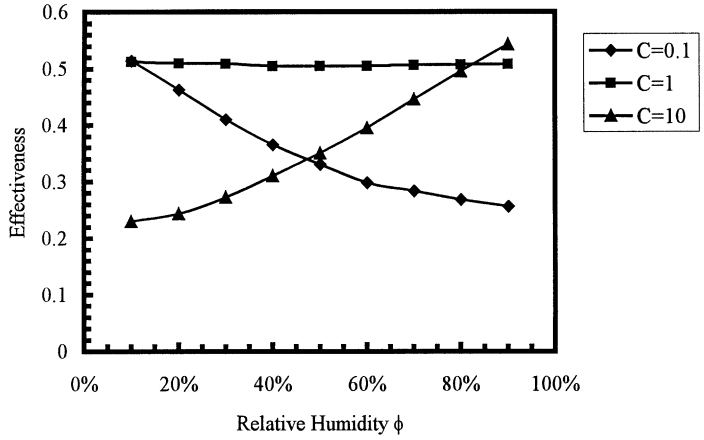

Fig. 10. Effects of relative humidity of supply air on effectiveness with supply in temperature (35°C).

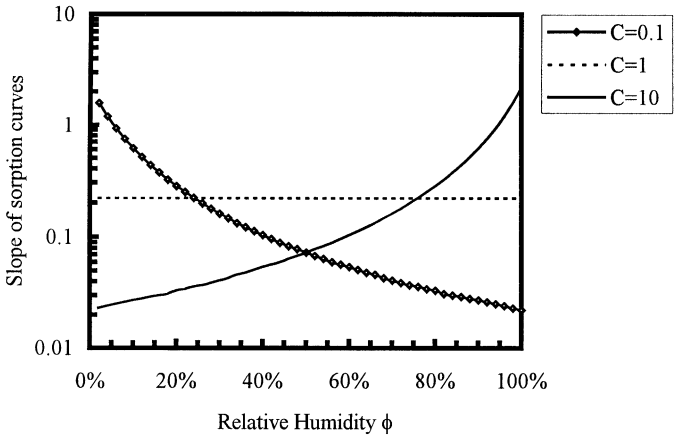

Fig. 11. Slopes of three types of sorption curves, type-I, $C = 0.1$; linear-type, $C = 1$; type-III, $C = 10$.

larger than the slopes of other materials, except at extremely humid or dry conditions. To help explain this reason, the slopes of the most commonly used three types of sorption curves are shown in Fig. 11.

From Fig. 11, it is clear that the slopes of the linear sorption curve are a constant. The slopes of the type-I sorption curve decrease with increasing relative humidity. In contrast, the slopes of the type-III sorption curve rise with relative humidity. The two slope curves meet together at 50% RH. For the relative humidities most commonly encountered in air conditioning, linear sorption material has the steepest slope.

3.2.4. *Effects of moisture uptake capacity* w_{max}

Fig. 12 shows the influences of the maximum moisture uptake of membrane material ($w_{\max}$) on latent effectiveness. The bigger the $w_{\max}$, the higher the latent effectiveness. This rule holds for all types of material. This is because a bigger $w_{\max}$ will result in higher moisture flow rate through the membrane. As a result, in practice, the moisture sorption potential is an index for selecting membrane materials. The higher the quantities of moisture adsorbed by a material, the better.

Shown in Fig. 13 is the variations of sensible, latent, and enthalpy effectiveness against different inlet air temperatures. The sensible effectiveness do not change much with supply air inlet temperature, while the latent effectiveness is very sensitive to temperature, especially when the temperature is bigger than

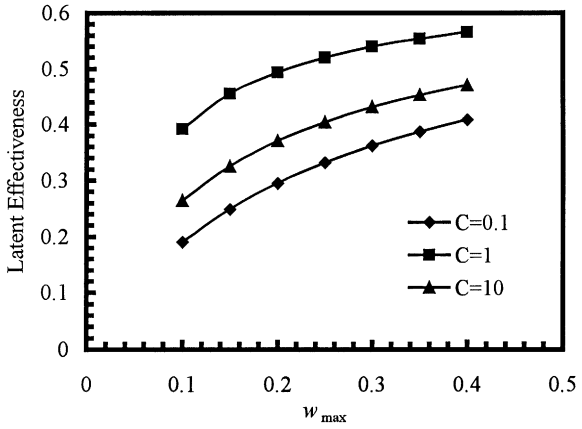

Fig. 12. Effects of maximum moisture uptake on latent effectiveness.

15°C. It decreases with rising temperatures. This is mainly due to increases in moisture resistance, which will be discussed in detail later. All membrane materials are similar in this respect.

3.3. *Clarification of the moisture transfer resistance for membrane*

The above discussions indicate that compared to heat transfer, moisture transfer through a membrane is more complicated and strongly coupled to operating conditions. To give a better understanding of the mois-

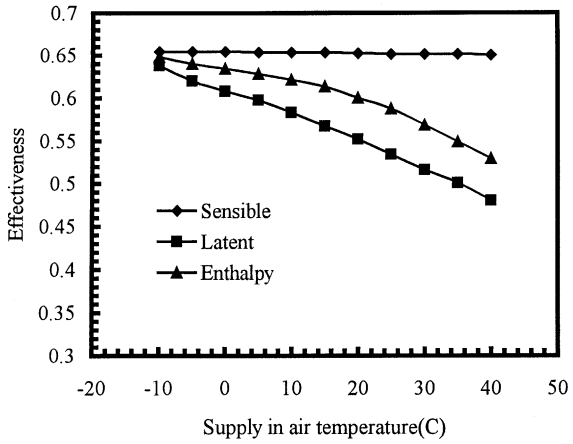

Fig. 13. Effects of supply air temperature on effectiveness.

ture transfer mechanisms through the membrane, it is imperative to study, rather, to clarify the moisture resistance in a membrane-based enthalpy exchanger. A more rational method may be to summarize the moisture resistance in a form similar to thermal resistance, like Eq. (35).

The moisture flow rate through the membrane

$$\dot{m}_W = k_s(\omega_s - \omega_{ms}) = k_e(\omega_{me} - \omega_e) \tag{41}$$

From Eq. (6), we have

$$\dot{m}_w = \frac{D_{wm}}{\delta}(\theta_{ms} - \theta_{me}) \tag{42}$$

$$\theta_{me} = \theta_{ms} + \left.\frac{\partial\theta}{\partial\phi}\right|_{ms} \Delta\phi = \theta_{ms} + \left.\frac{\partial\theta}{\partial\phi}\right|_{ms} (\phi_{me} - \phi_{ms}) \tag{43}$$

Substituting Eq. (43) into Eq. (42), we have

$$\dot{m}_W = \frac{D_{wm}}{\delta}\left(\frac{\partial\theta}{\partial\phi}\right)_s (\phi_{ms} - \phi_{me}) \tag{44}$$

Using Clapeyron equation to represent the saturation vapor pressure and assuming a standard atmospheric pressure of 101 325 Pa gives the relation between humidity and relative humidity as

$$\frac{\phi}{\omega} = \frac{e^{5294/T}}{10^6} - 1.61\phi \tag{45}$$

where T is in K. The second term on the right side of the equation will generally have less than a 5% effect, thus, it can be neglected. The subscript "s" which means "in supply side" is omitted for simplicity in Eq. (45) and following.

Re-arranging Eq. (42) through (45), we have

$$\dot{m}_W = \frac{1}{\gamma_{tot}}(\omega_s - \omega_e) \tag{46}$$

where γ_{tot} is the total moisture transfer resistance. It is similar to the expression of thermal resistance

$$\gamma_{tot} = \frac{1}{k_s} + \gamma_m + \frac{1}{k_e} \tag{47}$$

where the first and the third term are the convective mass transfer resistance on the supply side and exhaust side, respectively. The second term γ_m, is the moisture diffusive resistance in membrane. It can be expressed as

$$\gamma_m = \frac{\delta}{D_{wm}} \frac{10^6}{e^{(-5294/T)}(\partial\theta/\partial\phi)_s} \tag{48}$$

The differentiation of Eq. (17) gives

$$\frac{\partial\theta}{\partial\phi} = \frac{w_{max}C}{(1 - C + C/\phi)^2\phi^2} \tag{49}$$

The Eq. (48) can be further simplified as

$$\gamma_m = \frac{\delta}{D_{wm}}\psi \tag{50}$$

$$\psi = \frac{10^6(1 - C + C/\phi)^2\phi^2}{e^{(5294/T)}w_{max}C} \tag{51}$$

For a given membrane, δ/D_{wm} is a constant. Its form is very similar to the expression of thermal diffusive resistance through a plate. But the real diffusive resistance for moisture transfer is (δ/D_{wm}) times a dimensionless coefficient ψ. Therefore, we call (δ/D_{wm}) the nominal moisture diffusive resistance. The coefficient ψ is a new dimensionless parameter, which reflects the effects of operating conditions on the mass diffusive resistance. This parameter is very important and it is defined as the coefficient of mass diffusive resistance (CMDR). Comparisons of Eqs. (35) and (47) reveal that compared to thermal resistance, the moisture resistance through a membrane can also be separated into two categories: convective resistance and diffusive resistance. However, in contrast with thermal diffusive resistance, the moisture diffusive resistance

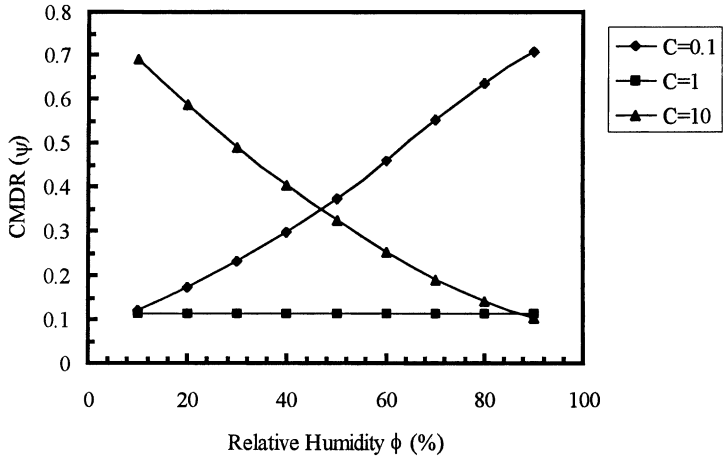

Fig. 14. Values of the coefficient of moisture diffusive resistance for three types of material under different humidities.

is not a constant. Rather, it is a variable co-determined by the nominal moisture diffusive resistance and the operating conditions.

It can be observed from Eq. (48) that even though temperature has an impact on the coefficient of moisture diffusive resistance, the most influential part comes from the slope of sorption curve. The steeper the sorption curve, the less the ψ and the mass transfer resistance. A less resistance then results in a higher performance.

The values of CMDR (ψ) under various humidities are calculated and shown in Fig. 14 for three types of materials. Note that the calculated value of CMDR is the log mean value across the whole membrane. For the linear sorption material, the CMDR is the least (0.12) and it does not change with humidity. However, the values of CMDR for the other two types of material vary considerably, inversely proportional to the respective slope curves. Generally speaking, the value of CMDR lies in the range of 0.12–0.70. The analysis of CMDR directly reveals why the linear sorption material is usually better than other materials. It also provides a key tool for moisture transfer analysis.

With the clarification and definition of diffusive resistance, it is now possible to evaluate the total resistance in moisture transfer and its effects on effectiveness. The effects of membrane diffusive resistance (γ_m) on the latent effectiveness are shown in Fig. 15. As can be seen, the latent effectiveness

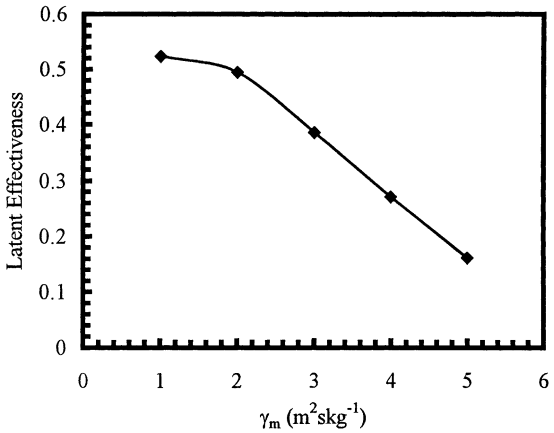

Fig. 15. Effects of diffusive resistance on latent effectiveness.

increases with a decrease in membrane diffusive resistance. However, when the resistance is smaller than $2.0\,m^2\,s\,kg^{-1}$, a further decrease of diffusive resistance has little merit in improving the effectiveness. The reason is that at this time, the diffusive resistance is already very small, and the total resistance of membrane is largely determined by the convective resistance, as shown in Eq. (47). This character is just similar to the effects of thermal resistance of a plate on the sensible heat exchanger effectiveness. Thus, to further increase moisture transfer, both the diffusive and the convective resistance should be reduced.

4. Conclusions

The sensible effectiveness of a membrane-based enthalpy exchanger is neither sensitive to membrane material nor to operating conditions. However, there is a strong coupling between the latent effectiveness and the membrane material and the operating conditions. The total moisture transfer resistance of membranes can be separated into convective and diffusive resistance. Unlike thermal diffusive resistance, the moisture diffusive resistance is not a constant. Rather, it is a function of the nominal diffusive resistance, sorption curves of material, and the operating conditions. However, a new dimensionless coefficient can be clarified and defined to summarize all these influences, which makes the analysis of coupled heat and moisture transfer in a membrane-based enthalpy exchanger easier. Nevertheless, material that could adsorb large quantities of water with a linear sorption curve is the best choice for enthalpy recovery.

Acknowledgements

This research is funded by the Research Grant Council of the Hong Kong SAR Government.

References

[1] ASHRAE, 1997 ASHRAE Handbook-Fundamentals, American Society of Heating, Refrigerating, and Air-Conditioning Engineers Inc., Atlanta, 1997.

[2] J.Y. San, Heat and mass transfer in a two-dimensional cross-flow regenerator with a solid conduction effect, Int. J. Heat Mass Transfer 36 (1993) 633–643.

[3] W.M. Worek, Z. Lavan, Performance of a cross-cooled desiccant dehumidifier prototype, ASME J. Solar Energy Eng. 104 (1982) 187–196.

[4] C.J. Simonson, R.W. Besant, Energy wheel effectiveness. Part I. Development of dimensionless groups, Int. J. Heat Mass Transfer 42 (1999) 2161–2170.

[5] C.J. Simonson, R.W. Besant, Energy wheel effectiveness. Part II. Correlations, Int. J. Heat Mass Transfer 42 (1999) 2171–2185.

[6] C.J. Simonson, R.W. Besant, Heat and moisture transfer in energy wheels during sorption, condensation, and frosting conditions, ASME J. Heat Transfer 120 (1998) 699–708.

[7] L.Z. Zhang, Y. Jiang, Heat and mass transfer in a membrane-based energy recovery ventilator, J. Membr. Sci. 163 (1999) 29–38.

[8] L.Z. Zhang, Y. Jiang, Y.P. Zhang, Membrane-based humidity pump: performance and limitations, J. Membr. Sci. 171 (2000) 207–216.

[9] J.Q. Wang, Z. Li, Synthesis of zeolite membrane and its application in removal of moisture from gases, Membr. Sci. Tech. 18 (1998) 54–58 (in Chinese).

[10] C.Y. Pan, C.D. Jensen, C. Bielech, H.W. Habgood, Permeation of water vapor through cellulose triacetate membranes in hollow fiber form, J. Appl. Polymer Sci. 22 (1978) 2307–2323.

[11] K. L Wang, S.H. Mccray, D.D. Newbold, E.L. Cusseler, Hollow fiber air drying, J. Membr. Sci. 72 (1992) 231–244.

[12] J.S. Cha, R. Li, K.K. Sirkar, Removal of water vapor and VOCs from nitrogen in a hydrophilic hollow fiber gel membrane permeator, J. Membr. Sci. 119 (1996) 139–153.

[13] M. Asaeda, L.D. Du, Separation of alcohol/water gaseous mixtures by thin ceramic membrane, J. Chem. Eng. Jpn. 19 (1986) 72–77.

[14] W.M. Kays, M.E. Crawford, Convective Heat and Mass Transfer, 3rd Edition, McGraw-Hill, New York, 1990.

[15] S.H. Chen, R.C. Ruaan, J.Y. Lai, Sorption and transport mechanism of gases in polycarbonate membranes, J. Membr. Sci. 134 (1997) 143–150.

[16] R. Taylor, R. Krishna, Multi-component Mass Transfer, Wiley, New York, 1993.